Altitude range resolution of differential absorption lidar ozone profiles

Georg Beyerle and I. Stuart McDermid

A method is described for the empirical determination of altitude range resolutions of ozone profiles obtained by differential absorption lidar (DIAL) analysis. The algorithm is independent of the implementation of the DIAL analysis, in particular of the type and order of the vertical smoothing filter applied. An interpretation of three definitions of altitude range resolution is given on the basis of simulations carried out with the Jet Propulsion Laboratory ozone DIAL analysis program, SO3ANL. These definitions yield altitude range resolutions that differ by as much as a factor of 2. It is shown that the altitude resolution calculated by SO3ANL, and reported with all Jet Propulsion Laboratory lidar ozone profiles, corresponds closely to the full width at half-maximum of a retrieved ozone profile if an impulse function is used as the input ozone profile. © 1999 Optical Society of America

OCIS codes: 010.3640, 010.4950, 280.1910, 280.3640, 350.5730.

1. Introduction

Differential absorption lidars (DIAL's) have been and continue to be widely used for the remote detection and monitoring of atmospheric trace gases such as ozone; see, e.g., Refs. 1–4. They now constitute an integral part of the Network for the Detection of Stratospheric Change (NDSC) for the long-term monitoring of stratospheric ozone. To achieve the goals of the NDSC, the ozone profiles supplied to the NDSC archive have been extensively verified in intercomparison campaigns; see, e.g., Refs. 5–7. However, uncertainty exists with respect to the interpretation of altitude resolutions reported by various ozone DIAL instruments.

In routine DIAL analysis, ozone number densities $n_{O_3}(z)$ are calculated by

$$n_{O_3}(z) = \frac{1}{\sigma_n - \sigma_f}\left\{\frac{1}{2}\left[\frac{\mathrm{d}}{\mathrm{d}z}\ln\frac{P_f(z)}{P_n(z)}\right] - [\alpha_n(z) - \alpha_f(z)]\right\}, \tag{1}$$

provided that the contribution from aerosol scattering can be neglected.[3,8,9] Here z is the geometric altitude; for on and off wavelengths λ_n and λ_f, $P_n(z)$ and $P_f(z)$ are the lidar signal counts at λ_n and λ_f, σ_n and σ_f are the ozone absorption cross sections, and α_n and α_f are the extinction coefficients for molecular scattering at λ_n and λ_f, respectively.

The evaluation of the term $\mathrm{d}/\mathrm{d}z\ \ln[P_f(z)/P_n(z)]$ is an essential element of the analysis. Generally, differentiation has the effect of applying a high-pass filter to a signal.[10] In DIAL analysis this fact represents a problem, as the signal counts $P_{n,f}(z)$ at stratospheric altitudes contain high-wave-number noise contributions. A straightforward replacement

$$\frac{\mathrm{d}}{\mathrm{d}z}f(z) \rightarrow \frac{f_{i+1} - f_{i-1}}{z_{i+1} - z_{i-1}} \quad \text{or} \quad \frac{\mathrm{d}}{\mathrm{d}z}f(z) \rightarrow \frac{f_i - f_{i-1}}{z_i - z_{i-1}} \tag{2}$$

would therefore amplify detector and statistical noise contributions more than the low-wave-number signal components that are due to ozone absorption and render the retrieved ozone profile useless.

Therefore stratospheric ozone DIAL algorithms, in most cases, employ a derivative smoothing filter that cuts off the high-frequency part of $P_{n,f}(z)$:

$$\frac{\mathrm{d}}{\mathrm{d}z}\ln\frac{P_f(z_i)}{P_n(z_i)} \rightarrow \sum_{j=-N(i)}^{N(i)} c_j(z_i)\ln\frac{P_f(z_{i+j})}{P_n(z_{i+j})}, \tag{3}$$

where c_j denote the filter coefficients of the derivative filter with order $M = 2N + 1$. As signal-to-noise ratios decrease for increasing altitude, the filter order

The authors are with the Table Mountain Facility, Jet Propulsion Laboratory, California Institute of Technology, P. O. Box 367, Wrightwood, California 92397. G. Beyerle is also affiliated with the Alfred Wegener Institute for Polar and Marine Research, Postfach 600 149, D-14401 Potsdam, Germany. The authors' email addresses are beyerle@tmf.jpl.nasa.gov and mcdermid@tmf.jpl.nasa.gov.

Received 4 May 1998; revised manuscript received 3 November 1998.

0003-6935/99/060924-04$15.00/0

and the filter coefficients are usually altitude dependent. A variety of different derivative filters have been described in the literature; see, e.g., Refs. 9 and 11–13.

Typically, the altitude resolution $\delta z(z_i)$ of ozone profiles is defined in terms of the derivative filter. Because various filters are used, values of $\delta z(z_i)$ from different data analyses are generally not comparable. Here we propose an empirical approach to determining $\delta z(z_i)$ that is independent of the particular filter used in the analysis program and can thus be applied to any DIAL analysis. The method is illustrated with simulations performed by SO3ANL, the Jet Propulsion Laboratory's stratospheric ozone DIAL analysis program. SO3ANL analyzes two pairs of signals, $P^L_{n,f}(z)$ and $P^H_{n,f}(z)$. Superscript L refers to the low-sensitivity channels (L channels) for ozone retrieval from 15 to 25 km, and superscript H to high-sensitivity channels (H channels) for altitudes from 25 to 50 km.

In SO3ANL a polynomial derivative filter of degree 1 is used; i.e., the filter coefficients are given by

$$c_j = \frac{3j}{N(N+1)(2N+1)}, \qquad j = -N, \ldots, N. \quad (4)$$

On the basis of extensive simulations the altitude dependence of the filter order $M = 2N + 1$ is parameterized as

$$M_L = 2(\max\{1.9396,\ 0.1871 \times \exp[9.1 \times 10^{-5}\ \mathrm{m}^{-1}(z - z_s)]\}^{1.046}) + 1,$$

$$M_H = 2(\max\{1.9396,\ 0.3741 \times \exp[9.1 \times 10^{-5}\ \mathrm{m}^{-1}(z - z_s)]\}^{1.046}) + 1$$

for the H (subscript H) and the L (subscript L) channels, respectively, z_s denotes the site altitude, and the boldface parentheses indicate rounding to the nearest integer.

2. Altitude Resolution

We determined the altitude resolution by performing a DIAL analysis with a simulated raw-data profile consisting of 1024 count values corresponding to the 1024 multichannel–scaler bins of the Jet Propulsion Laboratory stratospheric ozone lidar data-acquisition hardware. The detection channels operate in the photon-counting mode. The dwell time for each bin is 2 μs (corresponding to a step height of $\Delta z = 300$ m). Each simulated signal count profile was analyzed by SO3ANL in the same manner as for real data.

Two types of synthetic ozone profile, $\tilde{n}^{\mathrm{in}}$ and $\hat{n}^{\mathrm{in}}$, were used. One, $\tilde{n}^{\mathrm{in}}$, is a sine wave with wave number k and phase $0 \le \varphi < 2\pi$:

$$\tilde{n}^{\mathrm{in}}_j(z_i) = \frac{A}{2}\sin(2\pi k_j z_i + \varphi) + \frac{A}{2}, \quad (5)$$

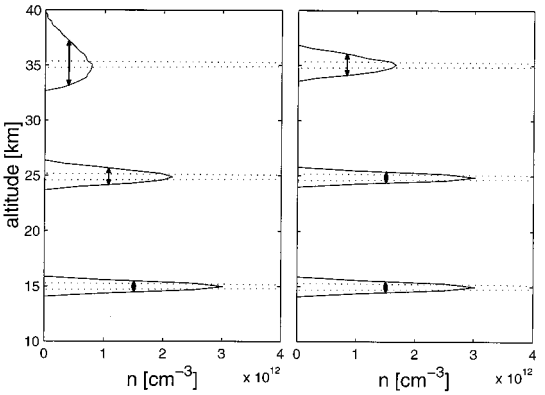

Fig. 1. Input (dotted curves) and retrieved output (solid curves) profiles for L-channel (left) and H-channel (right) analysis. The results for three impulse input functions, for $z_j = 15$ km, $z_j = 25$ km, and $z_j = 35$ km, are shown. The maximum of the input impulse function is 10^{13} cm^{-3}.

where $A = 10^{13}$ cm^{-3}. Adding the term $A/2$ ensures that $\tilde{n}^{\mathrm{in}}_j(z_i) \ge 0$. The other, $\hat{n}^{\mathrm{in}}$, is an impulse function:

$$\hat{n}^{\mathrm{in}}_j(z_i) = \begin{cases} A & z_i = z_j \\ 0 & \text{else} \end{cases}. \quad (6)$$

In what follows $\hat{n}^{\mathrm{out}}_j(z_i)[\tilde{n}^{\mathrm{out}}_j(z_i)]$ denotes the result obtained by SO3ANL for the synthetic input profile $\hat{n}^{\mathrm{in}}_j(z_i)[\tilde{n}^{\mathrm{in}}_j(z_i)]$. As an illustration, Fig. 1 shows $\hat{n}^{\mathrm{out}}_j(z_i)$ for three altitudes, $z_j = 15$ km, $z_j = 25$ km, and $z_j = 35$ km, analyzed as L-channel data (left) and H-channel data (right). For clarity the figure does not show the maximum of $\hat{n}^{\mathrm{in}}_j(z_i)$ (10^{13} cm^{-3}). Arrows indicate the full width at half-maximum of the results from the H- and L-channel analysis. The evident asymmetry of the $z_j = 35$ km profiles is caused by the exponential increase of filter order M with altitude. We note that in practice at 35 km the L-channel analysis data are not used.

Figure 2 shows $\tilde{n}^{\mathrm{out}}_j(z_i)$ and $\tilde{n}^{\mathrm{in}}_j(z_i)$ for a wave num-

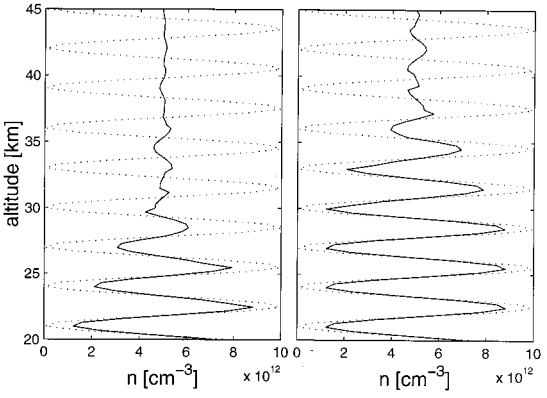

Fig. 2. Examples of input (dotted curves) and retrieved output (solid curves) profiles for L-channel (left) and H-channel (right) analysis. Here the wave number is 3 km^{-1}. Note the attenuation of the sine wave at higher altitudes and the phase shift between input and retrieved profiles from 42 to 44 km in the H-channel analysis.

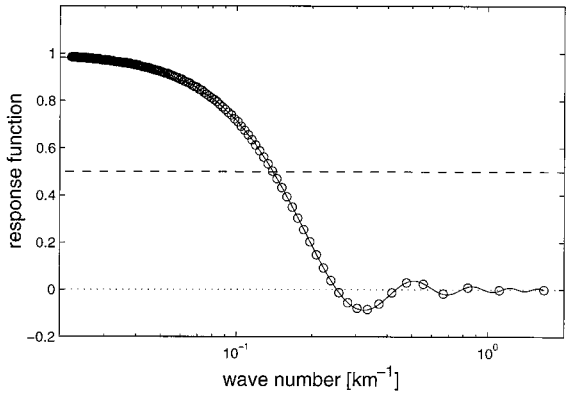

Fig. 3. Response function obtained by the SO3ANL simulation for filter order $N = 19$ (circles). The data are derived from the H data channels at altitudes from 41.7 to 42.6 km. For comparison the theoretically expected result is plotted as a solid curve.

ber of 3 km^{-1}. From 41- to 43-km altitude the H-channel data (dashed curve, right) $\tilde{n}_j^{\text{out}}(z_i)$ exhibit a phase shift of π with respect to $\tilde{n}_j^{\text{in}}(z_i)$. The cause for this phase shift is discussed below.

In what follows, we investigate three ways to calculate the altitude resolution δz that are used in DIAL algorithms[9,12,14,15]:

(1) $\delta z^{(1)} = 1/k_{1/2}$, where $k_{1/2}$ is the wave number for which the response function drops to 50%; i.e., $R(k_{1/2}) = 1/2$.

(2) $\delta z^{(2)} = M\,\Delta z$, where $\Delta z = z_{j+1} - z_j$ is the step height.

(3) $\delta z^{(3)}$, which is given by the full width at half-maximum of the retrieved profile $\hat{n}_j^{\text{out}}(z_i)$ if an impulse function $\hat{n}_j^{\text{in}}(z_i)$ is used as input.

As is shown below, these three definitions yield results that differ by as much as a factor of 2.

3. Results and Discussion

A total of 1651 simulated count profiles were analyzed by SO3ANL. For clarity no additional noise was added to $P_{n,f}(z)$. However, inasmuch as SO3ANL expects integer values for the signal counts, the simulated values $P_{n,f}(z)$ were rounded to the nearest integer, thereby producing quantization noise. One hundred fifty-one calculations were made with an impulse function with z_j, the location of the impulse, from 15 to 60 km and in steps of 300 m. One thousand five hundred simulations were performed with sine wave input profiles with wave numbers of 1/300, 1/600, and 1/900 m^{-1}, etc., decreasing to 1/45,000 m^{-1}. For each wave number, ten profiles with a random phase shift from 0 to 2π [relation (2)] were analyzed.

First we consider the sine input functions $\tilde{n}_j^{\text{in}}(z_i)$. For $\tilde{n}_j^{\text{in}}(z_i)$ we define a response function R by dividing the derived and input ozone profiles:

$$R(k_j, z_i) = \frac{\tilde{n}_j^{\text{out}}(z_i)}{\tilde{n}_j^{\text{in}}(z_i)}. \tag{7}$$

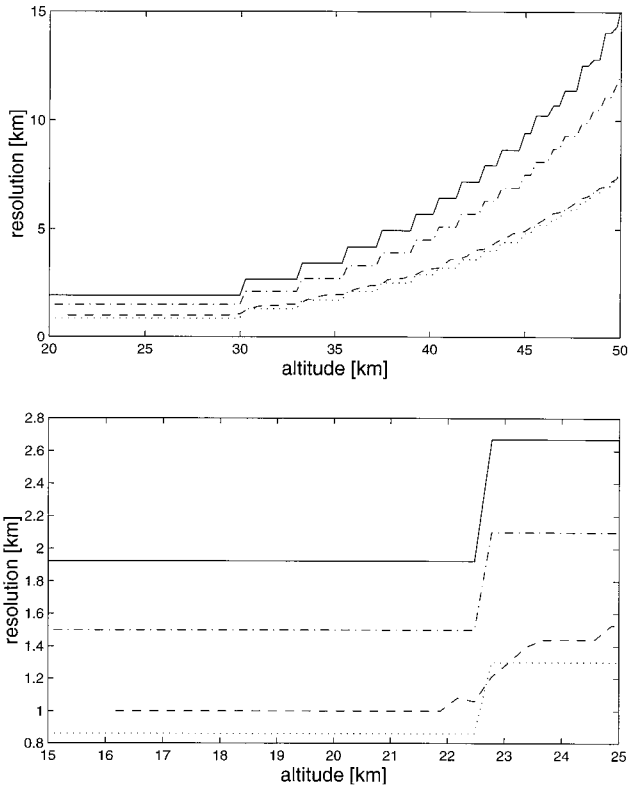

Fig. 4. Altitude resolutions $\delta z^{(1)}(z_i)$ (solid curves), $\delta z^{(2)}(z_i)$ (dashed–dotted curves), and $\delta z^{(3)}(z_i)$ (dashed curves) as a function of altitude for the low-sensitivity (top) and high-sensitivity (bottom) detection channels. The altitude resolutions calculated by SO3ANL are shown for comparison as dotted curves. The steplike pattern is caused by increases in the filter order.

R quantifies how strongly a sine wave ozone profile with wave number k is reduced. For $R(k, z) = 1$ the ozone profile is perfectly reproduced; for $R(k, z) = 0$ the corresponding sine wave component is completely suppressed in the retrieved profile. As an example of the results from the simulations, the response function for filter order $N = 19$ (corresponding to an altitude range 41.7–42.6 km, H-channel analysis) is shown in Fig. 3. At wave numbers larger than $k_{1/2} = 0.14$ km^{-1}, $R(k, z)$ falls below 0.5 (dashed line); i.e., for filter order $N = 19$ we obtain an altitude resolution of $\delta z^{(1)} = 7.1$ km. For comparison, the theoretically expected result

$$R(k) = \frac{1}{ik} \sum_{l=-N}^{N} c_l \exp(ilk) \tag{8}$$

obtained from the filter coefficients is plotted as well. Note that $\Im(R) = 0$ as $c_l = -c_{-l}$.

Figure 3 shows that $R(k)$ is negative [i.e., $\tilde{n}_j^{\text{in}}(z_i)$ and $\tilde{n}_j^{\text{out}}(z_i)$ are out of phase by π] for wave numbers from 0.25 to 0.43 km^{-1}. Figure 2 illustrates the effect of this phase shift in altitude space. At 41–44-km altitude $\tilde{n}_j^{\text{out}}(z_i)$ exhibits an ozone maximum where the input profile $\tilde{n}_j^{\text{in}}(z_i)$ has a minimum and vice versa.

We summarize the results of the simulations in Fig. 4, which shows the altitude resolutions $\delta z^{(1)}$,

$\delta z^{(2)}$, and $\delta z^{(3)}$ as functions of altitude. For comparison the altitude resolution obtained by SO3ANL is plotted as well. We find that altitude resolution reported by SO3ANL is in close agreement with $\delta z^{(3)}(z_i)$. Furthermore, the altitude resolutions $\delta z^{(1)}(z_i)$ and $\delta z^{(3)}(z_i)$ differ by approximately a factor of 2, whereas $\delta z^{(2)}(z_i)$ is $\sim$80% of $\delta z^{(1)}(z_i)$.

6. Conclusions

There is no unique definition for the altitude resolution of DIAL ozone profiles. The three definitions that we investigated were found to yield values that differ by as much as a factor of 2. For $\delta z^{(1)}$ and $\delta z^{(3)}$ an empirical approach to determining the altitude resolution can be used, which does not depend on the implementation of the DIAL analysis method.

We deliberately avoid discussion of the justifications for using or not using a certain definition of altitude resolution. The three definitions that we have studied here all have clear geophysical interpretations. However, we suggest that DIAL ozone data sets should contain information that defines the derivation of the altitude resolution reported.

Helpful discussions with M. R. Gross, T. J. McGee, J. J. Tsou, and P. von der Gathen are gratefully acknowledged. G. Beyerle thanks the National Research Council for the award of an associateship. The research described in this study was carried out at the Jet Propulsion Laboratory, California Institute of Technology, through an agreement with the National Aeronautics and Space Administration. This is contribution 1465 of the Alfred Wegener Institute.

References

1. O. Uchino, M. Maeda, J. Khono, T. Shibata, C. Nagasawa, and M. Hirono, "Observation of the stratospheric ozone layer by XeCl laser radar," Appl. Phys. Lett. **33,** 821–823 (1978).
2. J. Werner, K. W. Rothe, and H. Walther, "Monitoring of the stratospheric ozone layer by laser radar," Appl. Phys. B **32,** 113–118 (1983).
3. G. J. Megie, G. Ancellet, and J. Pelon, "Lidar measurements of vertical ozone profiles," Appl. Opt. **24,** 3454–3463 (1985).
4. I. S. McDermid, S. M. Godin, and L. O. Lindquist, "Ground-based laser DIAL system for long-term measurements of stratospheric ozone," Appl. Opt. **29,** 3603–3612 (1990).
5. I. S. McDermid, S. M. Godin, and T. D. Walsh, "Results from the JPL stratospheric ozone lidar during STOIC 1989," J. Geophys. Res. **100,** D5, 9263–9272 (1995).
6. W. D. Komhyr, B. J. Connor, I. S. McDermid, T. J. McGee, A. D. Parrish, and J. J. Margitan, "Comparison of STOIC 1989 ground-based lidar, microwave spectrometer, and Dobson spectrometer Umkehr ozone profiles with ozone profiles from balloon-borne electrochemical concentration cell ozone sondes," J. Geophys. Res. **100,** D5, 9273–9282 (1995).
7. J. J. Margitan, R. A. Barnes, G. B. Brothers, J. Butler, J. Burris, B. J. Connor, R. A. Ferrare, J. B. Kerr, W. D. Komhyr, M. P. McCormick, I. S. McDermid, C. T. McElroy, T. J. McGee, A. J. Miller, M. Owens, A. D. Parrish, C. L. Parsons, A. L. Torre, J. J. Tsou, T. D. Walsh, and D. Whiteman, "Stratospheric ozone intercomparison campaign (STOIC) 1989: overview," J. Geophys. Res. **100,** D5, 9193–9207 (1995).
8. R. M. Measures, *Laser Remote Sensing, Fundamentals and Applications* (Wiley, New York, 1984).
9. S. M. Godin, "Études expérimentale par télédétection laser et modélisation de la distribution verticale d'ozone dans la haute stratosphére," dissertation (Université Paris VI, Paris, 1987).
10. R. W. Hamming, *Digital Filters* (Prentice-Hall, Englewood Cliffs, N.J., 1989.
11. R. E. Warren, "Concentration estimation from differential absorption lidar using nonstationary Wiener filtering," Appl. Opt. **28,** 5047–5051 (1989).
12. T. Fujimoto and O. Uchino, "Estimation of the error caused by smoothing on DIAL measurements of stratospheric ozone," J. Meteorol. Soc. Jpn. **72,** 605–611 (1994).
13. W. Steinbrecht, "Lidar measurements of ozone, aerosol and temperature in the stratosphere," dissertation (York University, North York, Ontario, Canada, 1994).
14. T. J. McGee, NASA Goddard Space Flight Center, Greenbelt, Md. 20771 (personal communication, 1998).
15. J. J. Tsou, NASA Langley Research Center, Hampton Va. 23681 (personal communication, 1998).